KAVAKA 58 (4):10-17 (2022) DOI: 10.36460/Kavaka/58/4/2022/10-17

Eco-fabrication of anti-proliferative fluorescent silver nanoparticles using neem endophytic fungus

Ejaz Ahmad Siddiqui[1], Shadab Khan[1], Sahrish Arfin[1], Shruti Satpute[1], Pooja Salunkhe[1], Iqbal Siddiqui[1], Sk Najrul Islam[2], Renuka Bhor[3], Jyoti Otageri[3], Kalpana Pai[3], Narendra Kadoo[3], Vidya Gupta[3] and Absar Ahmad[*1,2]

[1]*Division of Biochemical Sciences, CSIR-National Chemical Laboratory, Pune-411008, India*

[2]*Interdisciplinary Nanotechnolcogy Centre (INC), Z.H. College of Engineering and Technology, Aligarh Muslim University, AMU, Aligarh, UP-202002, India.*

[3]*Department of Zoology, Savitribai Phule Pune University, Pune -411007, India.*

[*]*Corresponding author Email: aahmad786in@gmail.com*

(Submitted on September 22, 2022; Accepted on December 14, 2022)

ABSTRACT

Ever since scientists uncovered that plant-associated endophytic fungi have the ability to autonomously generate the same plant-based drugs/bioactive molecules; a multitude of endophytes have been utilized for the same. Extending the above aspect, our group directed it towards employing endophytes instead of plants in the 'eco-fabrication of nanoparticles'. The present manuscript demonstrates one such simple, reliable and ecological approach to the synthesis of biomedically and technologically prized silver nanoparticles (AgNPs) using an endophytic fungus isolated from neem (*Azadirachta indica* A. Juss.) leaves. Wet mycelial mass of the fungus when added to aqueous precursor silver nitrate ($AgNO_3$) led to the synthesis of profuse amounts of extracellular dispersed, fluorescent, quasi-spherical AgNPs of 20-60 nm having 20 nm average size. The nanoparticles were utterly characterized using recognized standard techniques. Cytotoxic activity of these nanoparticles was examined against human lung cancer cells (A549) and normal human peripheral blood mononuclear cells (PBMC), and it was observed that our AgNPs are anti-proliferative against cancer cells but safe toward normal cells. Furthermore, assessment of toxicity toward human RBCs (erythrocytes) revealed a mere 7% hemolysis in comparison to Triton X-100, consequently confirming the safe nature of our nanoparticles on human cells. Also, we scrutinized the anti-microbial potency of our biofabricated AgNPs and found them to be anti-microbial against different fungal (*Aspergillus niger*) and bacterial [Gram positive (*Bacillus subtilis* & *Staphylococcus aureus*), Gram negative (*Pseudomonas aeruginosa*)] strains. These multi-faceted nanoparticles will find broad spectrum applications in fields like drug/targeted delivery, therapeutics, theranostics, anti-microbial coatings, and so on

Keywords: Anti-microbial, Anti-proliferative, Eco-fabrication, Endophyte, Neem, Silver nanoparticles

INTRODUCTION

Since time immemorial, plants have been the central source for innumerable medicinal compounds; but in recent years, the tempestuous devouring of this transient resource has impaired it to frightfully low numbers. While trying to explore a suitable replacement, scientists uncovered that plant-associated endophytic fungi i.e. the ones which exist symbiotically within their host plants, have the ability to imitate the genetic-makeup of their specific hosts and fascinatingly, can autonomously generate the same plant-based drugs/bioactive molecules. Most of the plant materials which we eat have endophytes associated with them and these are harmless for human and animal consumption. This wonderful notion of intergeneric genetic exchange between plants and mutually beneficial fungi was manifested firstly when the gibberellin biosynthesis pathway in both the endophytic fungi and higher plants was found to be identical up to GA_{12}. Since then, a multitude of endophytic fungi has been utilized in the synthesis of plant-based drugs (Nicoletti *et al.,* 2015; Kumar *et al.,* 2013). As an example, the *Taxus baccata* tree is spared because its anticancer drug 'Taxol' is now being generated independently by the endophytic fungi isolated from it (Sreekanth *et al.,* 2009). As an extension to the above, our group directed the idea of solely using endophytes instead of plants towards the 'eco-fabrication of nanoparticles' in which plant parts were and are still amply used (Shankar *et al.,* 2003). Previously we had tested the synthesis of gold nanoparticles from both the leaves of geranium (*Pelargonium graveolens*) plant and from its endophytic fungus (*Colletotrichum* sp.) as well. Albeit the formation of stable gold nanoparticles was very speedy in both cases, still, the form and structure of the nanoparticles were contrasting; the endophyte yielded spherical gold NPs whereas the leaves generated several different shapes including rods, flat sheets and triangles (Shankar *et al.,* 2004). Our group is the key contributor to the green synthesis of various nanomaterials using endophytic fungi (Ahmad *et al.,* 2007; Bansal *et al.,* 2006; Bharde *et al.,* 2006; Islam *et al.,* 2022; Senapati *et al.,* 2014). This 'biological' method of nanoparticle fabrication weighs over the 'synthetic' chemical and physical protocols as it is non-toxic, occurs at ambient conditions of temperature, pressure and pH, is cheap, rapid and reliable. To add to this, the nanoparticles get capped by natural proteins secreted by the fungus during the process, granting them indispensable properties like non-aggregation, water dispersal, high stability and shelf-life, and nullifying the obligatory external capping agents which are mainly toxic as noticed in chemical and physical nano-manufacturing protocols.

An awe-inspiring rise in the research being performed upon silver nanoparticles has been witnessed in the past two decades, a testimonial to the deeply engrossing anti-diabetic, optical, conductive, thermal and electronic attributes displayed by these (Balan *et al.,* 2016; El-Aswar *et al.,* 2019; Guo *et al.,* 2019). Silver nanoparticles are extensively used for anti-microbial coatings on biomedical devices, wound dressings, skin grafts, cosmetics, clothing, footwear, paints, etc. and as inner surface coatings on household appliances like air conditioners, vacuum cleaners, washing machines, etc. where these unceasingly provide an overall anti-bacterial and anti-fungal outcome (Bocate *et al.,* 2019; Keshari *et al.,*

2020). Their large surface area allows for coordinating a plethora of ligands, making them apt for various areas of application like drug/targeted drug delivery, therapeutics, theranostics and so forth. Moreover, silver nanoparticles can independently penetrate bacterial cells causing serious morphological and structural changes, which can inhibit DNA replication and ultimately lead to cell death (Zielinska *et al.,* 2018). These nanoparticles have demonstrated synergistic action with commercial antibiotics like neomycin, ampicillin, penicillin, tetracycline, etc. (Deng *et al.,* 2016). Their intense surface plasmon resonance (SPR) grants them strong absorption and novel optical scattering properties which make silver nanoparticles an exceptionally versatile material of choice in molecular diagnostics, photonic devices, biosensors, etc. Innate qualities like high electrical conductivity and low sintering temperatures render silver nanoparticles purposeful in photovoltaics, conductive inks, and in composites to enhance electrical and thermal conductivity (Ciesielski *et al.,* 2019). Culminated, all these intrinsic properties make silver nanoparticles one of the most extensively explored materials for biomedical and technological applications. Nevertheless, these nanoparticles when synthesized by solution-phase synthetic/chemical routes tend to easily flocculate in colloidal solutions, are eco-unfriendly, cumbersome and non-uniform in size dimensions (Iravani *et al.,* 2014; Khodashenas *et al.,* 2019). Unearthing newer and more reliable ecological procedures for the production of nanomaterials is a vital stride in the blossoming sphere of biomedical nanotechnology; and so in the current study, we made significant efforts to derive these in a secure and cost-effective way. In the first report of its kind, we have already demonstrated the biological extracellular fabrication of silver nanoparticles (AgNPs) of 5-15 nm dimensions by adding wet mycelial mass of snow-white colored *Fusarium oxysporum* to an aqueous solution of silver nitrate ($AgNO_3$) (Ahmad *et al.,* 2003). However, the nanoparticles were neither completely characterized nor checked for any applications whatsoever. Also, our group has already fabricated gold, silver and core shell nanoparticles using neem (*Azadirachta indica* A. Juss.) leaf extracts (Shankar *et al.,* 2004). Presently, to refrain from the many seasonal, geographical and physical impediments which are faced while obtaining healthy material for research time and again, we isolated and purified many endophytic fungi from neem leaves collected from different areas in Pune city, India. A total of 58 endophytic fungi (EA-NEF: 1-58) were isolated and all were tested for silver nanofabrication. It was described that the culture EA-NEF:33 when added to aqueous precursor salt $AgNO_3$ produced profuse amounts of extracellular well dispersed AgNPs in the size range of 20-60 nm. The nanoparticles were utterly characterized using recognized standard techniques. The fungus was identified as *Fusarium oxysporum* based on cultural and morphological characteristics but texture wise appeared quite distinct from our earlier encounters, was light-yellow in color and imparted a pink pigment in the growth medium.

We carried out cytotoxicity studies on human lung cancer (A549) cells and normal human peripheral blood mononuclear cells (PBMC), where it was found that these biosynthesized AgNPs are anti-proliferative against cancer cells and safe for normal cells. As it is fundamentally confirmed that cancer cells lack DNA repair pathway as compared to normal cells, it implies that cell restoration could be compensated in normal cells in vivo conditions. Furthermore, assessment of toxicity toward human RBCs (red blood corpuscles/erythrocytes) revealed a mere 7% hemolysis in comparison to Triton X-100, consequently demonstrating the safe nature of our nanoparticles on human cells.

Microbial resistance to conventional drugs has upsurged globally. The presently available antibiotics cannot curb these drug resistant microorganisms and this ordeal is a lurking threat to mankind. Prime development of new therapeutic agents with efficacious antimicrobial activity is our absolute requisite; and thus, we scrutinized the anti-microbial potency of our biofabricated AgNPs. Filter paper bioassays were performed for the fungus Aspergillus niger and different bacterial strains [Gram positive (Bacillus subtilis & Staphylococcus aureus) and Gram negative (*Escherichia coli*)] whereupon our AgNPs exhibited significant antimicrobial activity, thereby proposing their prodigious potential to be developed as novel therapeutic agents.

MATERIALS AND METHODS

Materials

Silver nitrate ($AgNO_3$) was procured from Sigma Aldrich, USA and served as the precursor salt in the preparation of 10^{-3} M stock solution in distilled water. Components of MGYP media viz. malt extract, glucose, yeast extract and peptone were obtained from HiMedia Pvt. Ltd., India and used as received. Agar-agar was acquired from Fishers Scientific, USA.

Biological synthesis of Ag nanoparticles

The endophytic fungus EA-NEF:33 which was isolated from the leaves of *Azadirachta indica* A. Juss. was maintained on potato-dextrose-agar (PDA) slants at 25°C. for the bio-synthesis experiment, the fungus was grown in MGYP media composed of malt extract (0.3%), glucose (1.0%), yeast extract (0.3%) and peptone (0.5%) at 25-28 °C under shaking condition (200 rpm) for 96 h. Using sterile distilled water, the culture broth was centrifuged thrice under sterile conditions at 6000 rpm for 30 min at 15°C to wash and separate the mycelia. Harvested mycelia (25g) were resuspended into

1mM $AgNO_3$ solution in 500 ml Erlenmeyer flasks at pH7 and incubated on a shaker at 200 rpm. The reaction was carried out for 7 days, all through which the reaction mixture was visually inspected for color changes and monitored by UV-Visible spectroscopy measurements. After 7th day, the reaction mixture was filtered under sterile conditions using Whatman No.1 filter paper and lyophilized. The as-synthesized silver nanoparticles were then characterized using Transmission Electron Microscopy (TEM), Selected Area Electron Diffraction (SAED), X-ray Diffraction (XRD) and Fourier Transform Infrared (FTIR) spectroscopy. Their antimicrobial potential against bacteria (both Gram positive and Gram negative bacteria) and the fungus was tested in addition to cytotoxicity studies on cancer and normal cells. The fungus was identified to be *Fusarium oxysporum* based on cultural and morphological characteristics.

Characterization of Ag Nanoparticles

UV-visible spectroscopy : The bioreduction of $AgNO_3$ in solution was monitored by periodic sampling of aliquots (1 ml) of the aqueous component and measuring the UV-Visible spectra of the solution. Due to the high optical density of the nanoparticle solution, upto 20 times dilution was often required before the analysis. UV-visible spectra of these aliquots were monitored as a function of time of reaction using the Perkin Elmer UV-Vis-NIR spectrophotometer (Lambda 750) operated at a resolution of 1nm.

Fluorescence spectroscopy: Aliquots of the reaction mixture were subjected to fluorescence measurements carried out using a Perkin-Elmer LS 55 fluorescence spectrometer with a slit width of 10 nm and excitation at 420 nm.

Transmission electron microscopy (TEM): Samples for TEM analysis was prepared by drop coating biosynthesized AgNPs solution on carbon-coated copper TEM grids. The film on the TEM grid was allowed to stand for 2 minutes, after which the extra solution was removed and the grid was allowed to dry prior to measurement. TEM measurements were performed on a FEI Technai G2 system operated at an accelerating voltage of 200 kV at room temperature. The Selected Area Electron Diffraction (SAED) analysis was carried out on the same grid.

X-ray diffraction (XRD) measurements: To assess the crystal structure, thin films of the nanoparticles were drop casted on glass substrates and then subjected to X-ray diffraction analysis and data was recorded on Panalytical 'X' Pert PRO system operating at 40 kV and at a current of 30 mA with Cu Kα radiation (= 1.5404 Å).

Fourier transform infrared (FTIR) spectroscopy: The biological synthesis of nanoparticles involves protein mediated synthesis in the reaction mixture. These secreted proteins cap the AgNPs and provide water dispersibility and non-flocculation, and to further confirm this finding, FTIR analysis was performed on a Bruker Tensor 27 FTIR-ATR operated in the diffuse reflectance mode at a resolution of 4 cm^{-1}. To obtain good signal to noise ratio, 40 scans of the sample were taken in the range of 650-3500 cm^{-1}.

Antimicrobial activity

The bacterial cultures *Bacillus subtilis* (NCIM 2063), *Staphylococcus aureus* (NCIM 2079) and *Escherichia coli* (NCIM 2065) used for the antimicrobial activity were from our in house culture collection unit, the National Collection of Industrial Microorganisms (NCIM), Pune, India and the fungal culture *Aspergillus niger* was previously isolated in our lab itself. The antimicrobial activity of AgNPs was evaluated by filter paper bioassays. The bacterial cultures were inoculated in nutrient broth and incubated at 37˚C for 24 h. From the actively growing bacterial culture broth, 0.1 ml of bacterial suspension with a concentration of 10^5 CFU/ml was mixed with half strength nutrient broth (0.9 ml), immediately overlaid on the surface of sterile nutrient agar plates (90 mm diameter) and incubated at 37˚C for some time for initial growth. The exact method was followed for fungal cultures but MGYP-agar plates were used instead of nutrient agar. Sterile filter paper (Whatman No.3: 1 cm^2) pieces were placed on agar plates and loaded with 100 µl suspension of nanoparticles; suspension wasn't loaded for control. The plates were incubated for 24 h (48 h for fungus) and visually monitored for zone of inhibition. Post-incubation, the zone of inhibition was measured in millimeters across the filter paper.

Cytotoxicity studies

Cell culture and reagents: Human lung cancer (A549) cells were obtained from the National Centre for Cell Sciences (NCCS), Pune, and cultured in RPMI-1640 medium (Invitrogen) supplemented with 10% fetal bovine serum alongwith 100 µ/ml penicillin and streptomycin. All cells were grown in humidified atmosphere with 5% CO_2 and 95% air at 37°C. MTT dye was purchased from Himedia and Ficoll-paque from GE Healthcare, India.

Cell viability assay: Human lung cancer (A549) cells (2×10^4) were seeded in 96 well plates. Cells were treated with biosynthesized AgNPs for 24h with indicated concentration. Cell survival was determined by the modified MTT method (Sharma *et al.,* 2019). Treatment was terminated by removing media and MTT [3-(4,5-dimethylthiazol-2yl)-2,5-diphenyl tetrazolium bromide] (0.2 mg/ml) was added. After 4 h, crystals were dissolved in DMSO and absorbance was recorded at 570 nm.

Preparation of peripheral blood mononuclear cells (PBMC): Human PBMC were separated from heparinised, pooled whole blood of two healthy volunteers by Ficoll-paque gradient centrifugation (Ha *et al.,* 2020). Interface cells were collected and washed three times with PBS (pH 7.2),

counted and resuspended in RPMI medium. The protocol of the study was approved by the Ethics Committee of the University of Pune (Ethics-UoP/2012/19). Written informed consent was obtained from each healthy donor.

Cytotoxicity assay : PBMC (2×10^4 cells/ml) in RPMI were seeded in 96-well microtiter plates. After 30 min, cells were treated with AgNPs for 24h with indicated concentration added to the individual wells, in triplicate, except the wells for control. Ethanol was used as a vehicle control. Cell survival was determined by the modified MTT method of Mosmann (1983) Briefly, after the treatment with AgNPs for 24h, MTT solution (3-(4,5-dimethylthiazol-2-yl)-2,5-dyphenyl tetrazolium bromide) was added to each well. Samples were incubated for a further 4h, followed by the addition of 100 µl of DMSO and measurement of absorbance at 570 nm.

Haemolysis assay

Percent haemolysis of human RBCs (red blood cells/ erythrocytes) treatment with AgNPs was assessed by haemolysis assay as per US FDA Guidelines (FDA, 2005). RBCs were obtained from heparinised, pooled whole blood of two healthy volunteers, repeatedly washed with saline (pH 7.4). Thereafter, 1% RBC suspension was prepared and the subsequent erythrocyte suspension was incubated at 37°C for 1 h with different concentrations of the AgNPs or respective positive controls (1% Triton X-100) and vehicle control (Phosphate buffered saline). Following incubation, the samples were centrifuged at 400×g for 10 min and the absorbance of the supernatant was read at 540 nm in a spectrophotometer. Percent haemolysis was determined following comparison with 100% lysed erythrocytes.

Statistical analysis

The data reported in cytotoxicity and hemolysis experiments are expressed as mean±S.E. Statistical differences were determined by Student's t test. The p value < 0.05 was considered significant.

RESULTS AND DISCUSSION

The fungus EA-NEF:33 identified as *Fusarium oxysporum* (**Fig. 1A**) based on cultural and morphological characteristics (Hafizi *et al.,* 2013), when incubated with aqueous solution of 1mM $AgNO_3$, at temperature 25ºC and pH 7 for 7 days under shaking condition on a rotary shaker (200 rpm), resulted in the production of extracellular, water dispersible AgNPs. The change in color from colorless to brown (after 7 days) and the optical characteristics indicate the formation of Ag nanoparticles in reaction mixture **(Fig. 1B&C). Fig. 1D** shows the fungal biomass growing in MGYP medium. Extracellular nature of the produced nanoparticles was confirmed by simple filtration form the biomass. The AgNPs produced by EA-NEF:33 are capped by natural protein layer, which prevents cluster formation, thereby maintaining their

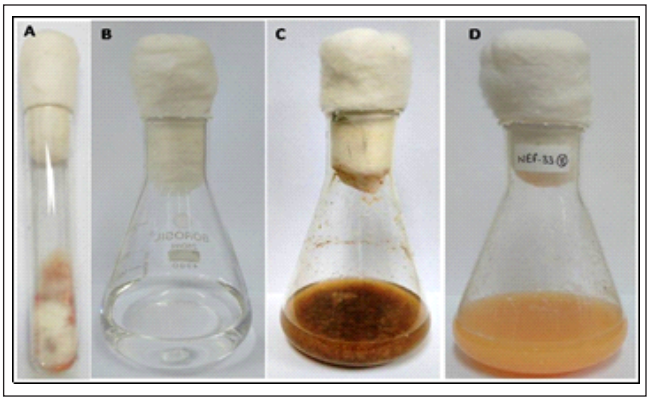

Fig. 1: (A) Fungus EA-NEF:33/*Fusarium oxysporum* (B) Precursor solution (1 mM $AgNO_3$), (C) Flask showing AgNPs generation (brown color). (D) Fungus growing in medium.

size and rendering them water dispersible. These natural proteins may aid in direct binding to multiple receptors like LHRH (luteinizing hormone-releasing hormone), EGFR (epidermal growth factor receptor) and EpCAM (epithelial cell adhesion molecule), folic acid, etc. nullifying the obligatory external target molecules as noticed in nanoparticles synthesized by physiochemical nanosynthesis routes.

Fig. 2A represents the UV-visible spectrum of biosynthesized silver nanoparticles. The spectrum clearly depicts the presence of characteristic nano silver SPR band at 410nm. The peak at 265nm can be attributed to the presence of aromatic amino acids such as tryptophan, tyrosine and phenylalanine in the sample containing silver nanoparticles. These aromatic amino acids can be originated from the proteins (secreted by the fungus while reacting with silver nitrate solution) associated with the biosynthesized silver nanoparticles which may be responsible for the reduction of Ag+ ions into silver nanoparticles and subsequent capping of the obtained silver nanoparticles. The inset in the figure shows two vials under day light containing colorless silver nitrate solution (1) and brown colored biosynthesized silver nanoparticles (2).

The fluorescence spectrum of so-formed silver nanoparticles is depicted in **Fig. 2B**. These biosynthesized silver nanoparticles when excited at 420 nm gave emission at 485 nm. It is well known fact that the three aromatic amino acids such as tryptophan, tyrosine and phenylalanine are responsible for the inherent fluorescence of proteins. We have already shown (**Fig. 2A**) the presence of these three aromatic amino acid residues in biosynthesized silver nanoparticles. We believe that the proteins/protein comprises of these amino acid residues are responsible for the capping and also imparting characteristic fluorescence to biosynthesized silver nanoparticles. The inset shows silver nitrate solution (1) and fluorescent biosynthesized silver nanoparticles (2) upon

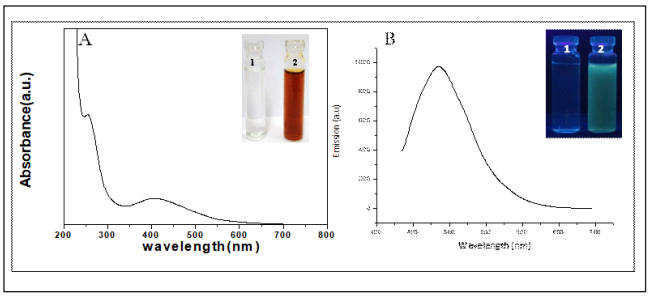

Fig. 2: UV-Visible spectrum (A) and fluorescence spectroscopy analysis (B) of biosynthesized AgNPs. The insets in figures A and B show two vials containing silver nitrate solution (1) and so-formed silver nanoparticles (2) under day light and under UV lamp illumination respectively.

illumination by UV lamp at 365 nm, thus depicting the remarkable potential of these nanoparticles to be developed as a diagnostic and imaging agent.

TEM analysis was performed to monitor the size and shape of the so-formed AgNPs (**Fig. 3A-B**). The morphology of the synthesized nanoparticles is quasi-spherical with size dimensions of 20-60 nm. These nanoparticles are capped by natural proteins and are well dispersed as evident from the TEM micrograph. **Fig. 3C** depicts the particle size distribution of biosynthesized silver nanoparticles calculated from **Fig. 3A** (by calculating 100 particles, n=100). The average size of the silver nanoparticles was found to be 20 nm. SAED (**Fig. 3D**) pattern shows crystalline nature of the nanoparticles. The minuscule size of these nanoparticles makes them very suitable for anti-microbial gels, drug delivery, etc. without chances of toxicity as these may be filtered through the kidneys and excreted through urine.

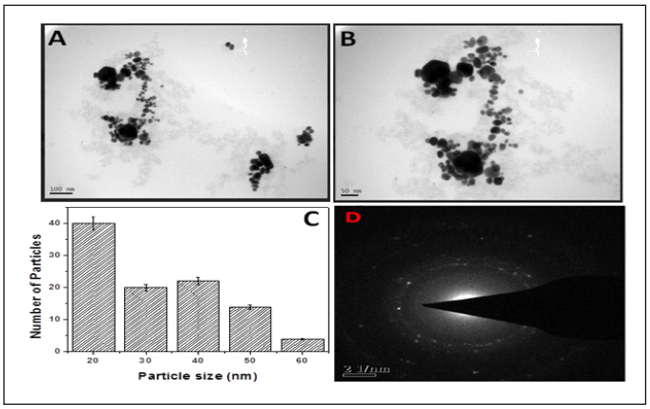

Fig. 3: TEM images of biosynthesized silver nanoparticles at different magnifications (A&B), Particle size distribution (C) and SAED pattern of silver nanoparticles (D).

Fig. 4A represents the X-ray diffraction (XRD) analysis of biosynthesized silver nanoparticles. The diffractogram shows Bragg's reflection corresponding to the planes (111), (200), (220) and (311) which can be indexed with the PCPDF card number (40783) which is the standard XRD pattern for AgNPs.

Fig. 4B represents the FTIR analysis of biosynthesized silver nanoparticles. The FTIR spectrum shows the presence of two peaks at 1590 and 1395 cm^{-1} which can be attributed to amide I and amide II respectively (Syed *et al.,* 2014) of the proteins associated with silver nanoparticles. We believe that these proteins/proteins are responsible for the synthesis and capping of biosynthesized silver nanoparticles.

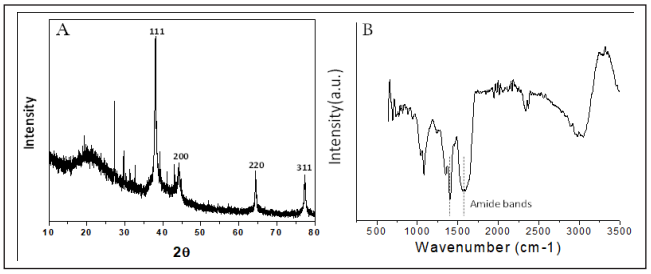

Fig. 4: X-ray diffraction pattern (A) and FTIR measurement of biosynthesized AgNPs (B).

To know the proteins responsible for the synthesis of silver nanoparticles SDS-Polyacrylamide Gel Electrophoresis (SDS-PAGE) was carried out at pH 8.3 (Velmurugan *et al.,* 2014). We have loaded the as synthesized silver nanoparticles in lane B and protein molecular markers in lane A. The gel was stained by Coomasie Brilliant Blue R 250. From the **Fig. 5** it is clear that the silver nanoparticles consist of two proteins

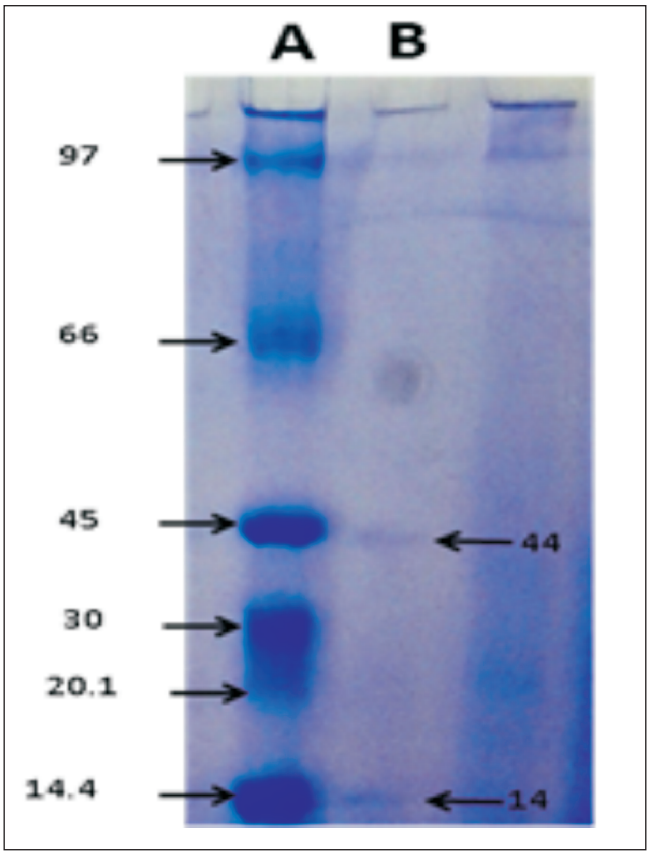

Fig. 5: SDS-PAGE analysis of biosynthesized silver nanoparticles. Lane A was loaded with protein molecular markers and Lane B was loaded with silver nanoparticles.

which correspond to 44 and 14 kDa respectively. We believe that the 44 kDa protein is responsible for the reduction of silver ions into nanosilver and the low molecular weight protein i.e. 14 kDa is responsible for the capping of the obtained silver nanoparticles. Kumar *et al.* (2007) have also reported the role of nitrate reductase enzyme with molecular weight of 44 kDa in the formation of silver nanoparticles (Kumar *et al.,* 2007).

Antimicrobial activity of the silver nanoparticles

Antimicrobial activity of the AgNPs synthesized using EA-NEF:33 was carried out against Gram positive (*Staphyllococcus aureus* and *Bacillus subtilis*) and Gram negative (*Escherichia coli*) bacterial strains and the fungus *Aspergillus niger*. The filter paper bioassay for antimicrobial activity showed a clear zone of inhibition developed around the filter paper disc against the bacterial growth of both Gram positive and Gram negative bacteria. The inhibition zone upon measurement was found to be most for *E. coli* followed by *S. aureus* and *B. subtilis* respectively. Zone of inhibition was also obtained in case of the fungus *A. niger* (**Fig. 6**). As our AgNPs have both antibacterial and antifungal activity, their broad-spectrum inhibitory action will be prevalent.

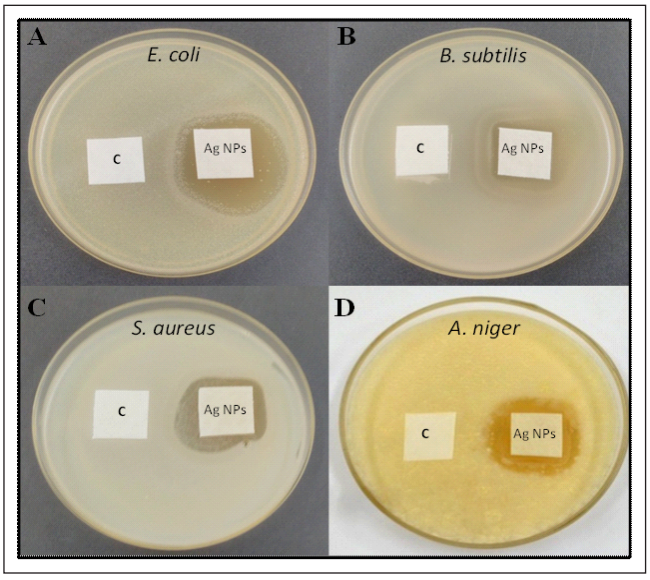

Fig. 6: Antibacterial activity of AgNPs against Gram negative bacteria (*E-coli*) (A), Gram positive bacteria [*Bacillus subtilis* (B) & *Staphylococcus aureus* (C)] and anti-fungal activity against fungus (*A. niger*) (D). The clearance zone obtained around the filter paper disc in all the plates clearly indicated the anti-microbial activity of so-formed AgNPs.

Cytotoxicity studies

Fig. 7A represents the cytotoxicity data of biosynthesized AgNPs against two different cell types viz. human lung cancer cells (A549) and normal human peripheral blood mononuclear cells (PBMC). The cytotoxicity against A549 was found to be about 75% (i.e. 25% viability) from 5-500 µg/ml conc. of biosynthesized AgNPs. Interestingly, PBMC, which are normal human cells, show highest cell viability (approx. 90%) with least cytotoxicity (approx. 10%) from the same concentration of above nanoparticles. This data suggest that our biosynthesized AgNPs are anti-proliferative against human lung cancer (A549) cells and show no adverse effect on normal (PBMC) cells, and so may serve as excellent vectors for drug delivery.

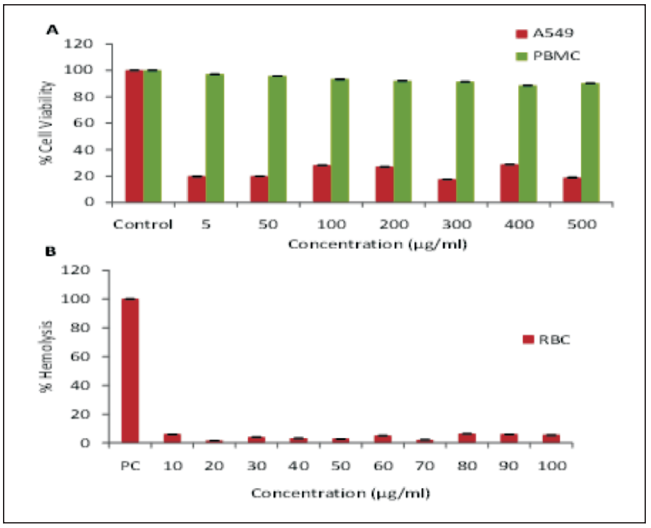

Fig. 7: Percent cell viability of A549 cells and PBMC against silver nanoparticles (A) and Percent hemolysis by silver nanoparticles (B); PC- positive control.

Percent cytotoxicity and hemolytic activity

Fig. 7B depicts the percent hemolysis data of human red blood cells (RBC). Our nanoparticles show only up to 7% hemolysis when used in a range from 10-100 µg/ml concentration. This data suggest that our biosynthesized AgNPs are compatible with RBCs and can be used in drug/targeted delivery applications without generating any harmful effects in the blood stream. Upon live observation under Phase Contrast Microscope (**Fig. 8**), A549 cells treated with medium alone (control) showed normal appearance as compared to the ones treated with so-formed AgNPs, whereby cells exhibited loss in normal architecture and cell death.

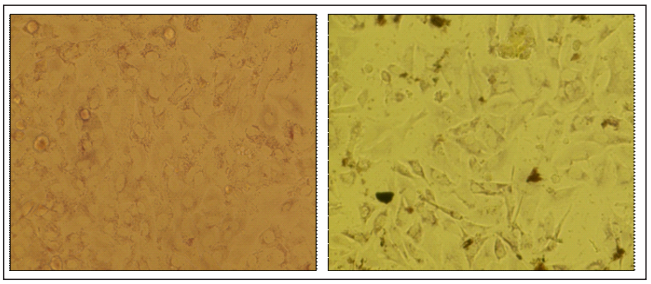

Fig. 8: Images of control/ untreated (left) and so-formed AgNPs treated (right) human lung cancer (A549) cells at 40X magnification under a Phase Contrast Microscope.

CONCLUSIONS

In this manuscript, we have shed light upon the potential of novel endophytic fungus (*Fusarium oxysporum*) isolated from neem leaves in the fabrication of biomedically and

technologically valuable silver nanoparticles. The process led to the synthesis of natural protein capped, water dispersible, very stable and fluorescent silver nanoparticles of 20-60 nm dimensions. These nanoparticles showcased excellent antimicrobial attributes and may serve as new antimicrobial agents at a time when microbial drug resistance (MDR) is skyrocketing. Cytotoxicity studies revealed the significant anti-proliferative potency of the biosynthesized silver nanoparticles against human lung cancer (A549) cells, while being very safe towards normal (PBMC) cells. Moreover, toxicity assessment toward human erythrocytes disclosed a mere 7% hemolysis as compared to Triton X-100, consequently entailing the safe nature of our nanoparticles. In summation, these qualities make our eco-fabricated silver nanoparticles a very versatile and dynamic material of choice in radical development of drug carriers, cosmetics, antimicrobial gels and coatings, therapeutics, theranostics and so forth.

ACKNOWLEDGMENTS

A.A. acknowledges the Department of Biotechnology (DBT), Government of India, for setting up a Centre of Excellence (COE, BT/PR1-3584/COE/34/29/2015) at the Interdiscipli-nary Nanotechnology Centre (INC), Aligarh Muslim University, AMU, Aligarh, UP-202002, India. AA also thank the Department of Biotechnology, Government of India (New Delhi) for the Tata Innovation Fellowship award and financial support through BSC0112-CSIR. S.K. thank CSIR for Research Associateship. KP is supported by ICMR grant. The authors thank Centre for Materials Characterization (CSIR-NCL) for assistance regarding TEM and XRD measurements.

REFERENCES

Ahmad, A., Mukherjee, M., Satyajyoti, S. *et. al.* 2003. Extracellular biosynthesis of silver nanoparticles using the fungus *Fusarium oxysporum*. *Colloids and Surfaces B: Biointerfaces.* **28:** 313-318.

Ahmad, A., Jagdale, T., Dhas, V. *et al.* 2007. Fungus based synthesis of chemically difficult to synthesize multifunctional nanoparticles of $CuAlO_2$. *Adv. Mater.* **19:** 3295-3299.

Balan, K., Qing, W., Wang, Y. *et al.* 2016. Antidiabetic activity of silver nanoparticles from green synthesis using *Lonicera japonica* leaf extract. *RSC Adv.* **6(46):** 401-628.

Bansal, V., Poddar, P., Ahmad, A. *et al.* 2006. Room-temperature biosynthesis of ferroelectric barium titanate nanoparticles. *J. Am. Chem. Soc.* **128:** 11958-11963.

Bharde, A., Rautaray, D., Bansal, V. *et al.* 2006. Extracellular biosynthesis of magnetite using fungi. *Small.* **2:** 135-141.

Bocate, K.P., Reis, G.F., de-Souza, P.C. *et al.* 2019. Antifungal activity of silver nanoparticles and simvastatin against toxigenic species of *Aspergillus*. *Int. J. Food Microbiol.* **291:** 79-86.

Ciesielski, A., Czajkowski, K.M. and Switlik, D. 2019. Silver nanoparticles in organic photovoltaics: Finite size effects and optimal concentration. *Sol. Energy* **184:** 47788.

Deng, H., McShan, D., Zhang, Y. *et al.* 2016. Mechanistic Study of the synergistic antibacterial activity of combined silver nanoparticles and common antibiotics. *Environ. Sci. Technol.* **50(16):** 8840-8848.

El-Aswar, E.I., Moustafa Moawad Zahran, M.M. and El-Kemary, M. 2019. Optical and electrochemical studies of silver nanoparticles biosynthesized by *Haplophyllum tuberculatum* extract and their antibacterial activity in wastewater treatment. *Mater. Res. Express.* **6(10):** 105016.

FDA, May 2005. *Guidance for Industry- Nonclinical Studies for the Safety Evaluation of Pharmaceutical Excipients Rockville*, MD.

Guo, Y., Yang, X., Ruan, K. *et. al.* 2019. Reduced graphene oxide heterostructured silver nanoparticles significantly enhanced thermal conductivities in hot-pressed electrospun polyimide nanocomposites. *ACS Appl. Mater. Interfaces* **11(28):** 25465-73.

Ha, M.K., Choi, J., Kwon, S.J. *et al.* 2020. Mass Cytometric Study on the Heterogeneity in Cellular Association and Cytotoxicity of Silver Nanoparticles in Primary Human Immune Cells. *Environ. Sci.: Nano.* **7:** 1102-1114.

Hafizi, R., Salleh, B. and Latiffah, Z. 2013. Morphological and molecular characterization of *Fusarium solani* and *F. oxysporum* associated with crown disease of oil palm. *Brazilian J. Microbiol.* **44(3):** 959-68.

Iravani, S., Korbekandi, H., Mirmohammadi, S.V. *et al.* 2014. Synthesis of silver nanoparticles: chemical, physical and biological methods. *Res. Pharm. Sci.* **9:** 385-406.

Islam, S.N., Raza, A., Naqvi, S.M.A. *et al.* 2022. Unveiling the antisporulant activity of mycosynthesized gold-selenide nanoparticles against black fungus *Aspergillus niger*. *Surfaces and Interfaces* **29:** 101-769.

Keshari, A.K., Srivastava, R., Singh, P. *et. al.* 2020. Anti-oxidant and antibacterial activity of silver nanoparticles synthesized by *Cestrum nocturnum*. *Ayurveda Integr. Med.* **11(1):** 37-44.

Khodashenas, B. and Ghorbani, H.R. 2019. Synthesis of silver nanoparticles with different shapes. *Arab J Chem.* **12(8):** 182-338.

Kumar, A., Patil, D., Rajamohanan. P. *et. al.* 2013. Isolation, purification and characterization of vinblastine and vincristine from endophytic fungus *Fusarium oxysporum* isolated from *Catharanthus roseus*. *Plos One.* **8:** e71805.

Kumar, S. A., Abyaneh M. K., Gosavi, S.W.S. *et al.* 2007. Nitrate reductase-mediated synthesis of silver nanoparticles from $AgNO_3$. *Biotechnol. Lett.* **29:** 439-445.

Mosmann, T. 1983. Rapid colorimetric assay for cellular growth and survival: application to proliferation and cytotoxicity assays. *J. Immunol. Methods* **65:** 55-63.

Nicoletti, R. and Fiorentino, A. 2015. Plant bioactive metabolites and drugs produced by endophytic fungi of spermatophyta. *Agriculture* 2015. **5:** 918-970.

Shankar, S., Ahmad, A., Pasricha, R. *et. al.* 2003. Bio-reduction of chloroaurate ions by geranium leaves and its endophytic fungus yields gold nanoparticles of different shapes. *J. Mater. Chem.* **13:** 1822-1826.

Shankar, S.S., Rai, A., Ahmad, A. *et al.* 2004. Rapid synthesis of Au, Ag, and bimetallic Au core-Ag shell nanoparticles using neem (*Azadirachta indica*) leaf broth. *Journal of Colloid and Interface Science* **275:** 496-502.

Shankar, S., Rai, A., Ankamwar, B. *et. al.* 2004. Biological synthesis of triangular gold nanoprisms. *Nature Materials* **3:** 482-488.

Sharma, V., Kaushik, S., Pandit, P. *et al.* 2019. Green synthesis of silver nanoparticles from medicinal plants and evaluation of their antiviral potential against chikungunya virus. *Appl. Microbiol. Biotechnol.* **103(2):** 88-191.

Sreekanth, D., Syed, A., Sarkar, S. *et. al.* 2009. Production, purification, and characterization of taxol and 10-DABIII from a new endophytic fungus *Gliocladium* sp. isolated from the Indian yew tree, *Taxus baccata*. *J. Microbiol. Biotechnol.* **19:** 1342-1347.

Senapati, S., Syed, A., Khan, S. *et. al.* 2014. Extracellular biosynthesis of metal sulfide nanoparticles using the fungus *Fusarium oxysporum*. *Curr. Nanoscience* **10:** 588-595.

Syed, B., Kumar, K.M., Santosh, P. *et al.* 2014. Extracellular synthesis of silver nanoparticles by novel *Pseudomonas veronii* AS 41G inhabiting *Annona squamosa* L. and their bactericidal activity. *Spectrochimica Acta. Part A, Molecular and Biomolecular Spectroscopy* **136(C):** 1434-1440.

Velmurugan, P., Iydroose, M., Mohideen, M.H.A.K. *et al.* 2014. Biosynthesis of silver nanoparticles using *Bacillus subtilis* EWP-46 cell-free extract and evaluation of its antibacterial activity. *Bioprocess Biosyst. Eng.* **37(8):** 152-734.

Zielinska, E., Zauszkiewicz-Pawlak, A., Wojcik, M. *et. al.* 2018. Silver nanoparticles of different sizes induce a mixed type of programmed cell death in human pancreatic ductal adenocarcinoma. *Oncotarget.* **9(4)**: 467-597.